Active Fault Structure and Potential High Temperature Geothermal Systems: Lidar Analysis of the Gabbs Valley, Nevada, Fault System

Jonathan Payne[1], John Bell[2], Wendy Calvin[1], and Karl Spinks[3]

[1]Geological Sciences and Engineering, University of Nevada, Reno
[2]Nevada Bureau of Mines and Geology, University of Nevada, Reno
[3]GeoGlobal Energy, Santa Rosa, California

Keywords

Seismically active faults, lidar, structural controls, blind geothermal, exploration tools

ABSTRACT

High temperature geothermal systems in the Great Basin have been linked to active Quaternary faults. Surface ruptures from two historical earthquakes, the 1932 Cedar Mountain (M_S 7.2) and 1954 Fairview Peak (M_S 7.2), overlap in the area of the Gabbs Valley, Nevada geothermal lease. New mapping of Quaternary faults is in progress utilizing low sun-angle aerial photography and Lidar remote sensing imagery. Holocene and historic fault ruptures record an actively deforming area and these faults are likely to have fractured, brecciated rock associated with their fault plane(s) at depth. Permeability associated with these fault planes is a potential geothermal fluid pathway.

High-resolution hill shade and slope shade images were generated from lidar (light detection and ranging) data collected by Watershed Sciences, Inc. for GeoGlobal Energy covering their BLM geothermal lease area near Cobble Cuesta in Gabbs Valley, Nevada. Bare earth digital elevation models (DEMs) were provided by Watershed Sciences with horizontal ground resolution of 0.5 m, and vertical accuracy better than 0.05 m. The synthetic images, along with low sun-angle (sun ~10-25° above the horizon) aerial photography (LSA) were used for detailed mapping of Quaternary fault scarps to a scale of 1: 3,000 or better. The use of hill shade, slope shade and LSA imagery provides a variety of methods and repeatability to identify fault scarps.

Detailed mapping depicts two fault trends. The Phillips Wash fault zone is primarily located in the wash between Cobble Cuesta (a low, broad ridge) and the Monte Cristo Mountains. These scarps are NNE striking and discontinuous. Fault segments exhibit a right stepping en echelon pattern and graben of varying size and extent. The Eastern Monte Cristo Mountains fault zone ruptures the piedmont alluvial fans striking NNE and increasing in fault zone width to the north. Typically the piedmont faults are relatively longer and more continuous. The longer length, increased height of scarps, and older ages of alluvial fan surfaces cut by these fault scarps records a longer paleoseismic history. Mapped fault data will be field verified and combined with kinematic data to discern current stress orientations at the site. Interpretations will be integrated into GeoGlobal's structural kinematic model for the resource.

Introduction

The Gabbs Valley geothermal prospect is a blind thermal anomaly located between the Paradise Range and Monte Cristo Mountains west of Gabbs, NV (Figure 1). Anomalous temperatures were identified in warm wells in Gabbs, NV and small ranches nearby. Hot springs are present on the west side of Fissure Ridge outside the lease. In the late 1970s, Al-Aquitaine Exploration, LTD completed temperature gradient drilling (51 holes to ~150 m) and geophysical studies identifying a thermal anomaly with temperature gradients exceeding 1° C/ 30 m over an area of approximately 40 km^2. Results of the survey indicated an association of the highest temperature wells with a NW striking fault identified by hypocenters of micro-seismic events and the presence of a broad, horizontal low-resistivity layer. These results are interpreted to indicate the geothermal system is controlled by active faulting and is capped by an impervious clay horizon. The 1970's survey identified a broad geothermal anomaly that is being revisited today with the goal of successfully targeting deep geothermal explorations wells to prove an economic resource.

Active Holocene fault scarps have been identified at 37 hot spring locations in the Great Basin and are associated with additional blind geothermal systems (Bell and Ramelli, 2009). Previous work modeling enhanced geothermal systems, and fault controlled geothermal systems have integrated active fault mapping, structural kinematic and slip data, and used stress inversion to identify faults oriented for maximum shear or dilation (Moeck et al., 2009; Moeck et al., 2010). As part of GeoGlobal Energy's (GGE) exploration plan a comprehensive structural conceptual model will be developed to identify preferential targets for deep exploration wells. Lidar and low sun-angle (LSA) aerial photos were acquired covering the area west of Fissure Ridge and the

Monte Cristo Mountains to the east shoulder of Cobble Cuesta. We will identify and map active faults in the area, and determine their sense of motion. Constraints on fault orientation and motion will provide necessary information for a structural conceptual model of the Gabbs thermal anomaly.

Background

Located adjacent to the Walker Lane Belt in the Basin and Range (Figure 1), the Gabbs Valley prospect is in a tectonically active area. The Basin and Range currently accommodates roughly east-west extension along steeply dipping N to NE striking normal faults (Stewart, 1978) while the Walker Lane Belt accommodates oblique dextral shear along steeply dipping NW to NNW striking faults (Stewart, 1988). Clockwise vertical block rotations, a result of dextral shear, have been documented in the Walker Lane (Cashman and Fontaine, 2000) and are associated with E-W striking sinistral faults that separate different domains (Stewart, 1988). Gabbs Valley is just east of the Walker Lake domain. Approximately 10 cm/yr dextral shear is accommodated in the Walker Lane and dies out to the north where shear strain is most likely transferred to Basin and Range extension (Faulds et al., 2005; Hammond and Thatcher, 2007). Just to the south of the prospect are the Petrified Springs and Benton Springs faults along the Gabbs Valley Range. These major structures are NW striking dextral strike-slip faults and have geologic slip rates of 1-2 mm/yr (Wesnousky, 2005). At the northern termination of these faults and to the east the structural grain changes from NW striking to NE striking ranges (Figure 1). The Gabbs Valley prospect is possibly controlled by strain transferred from the Walker Lane to the Basin and Range where much lower geologic slip rates of 0.2-0.5 mm/yr (Bell et al., 1999; Adams and Sawyer, 1999; Bell et al., 2004) have been determined for Quaternary faults near and south of Gabbs, NV.

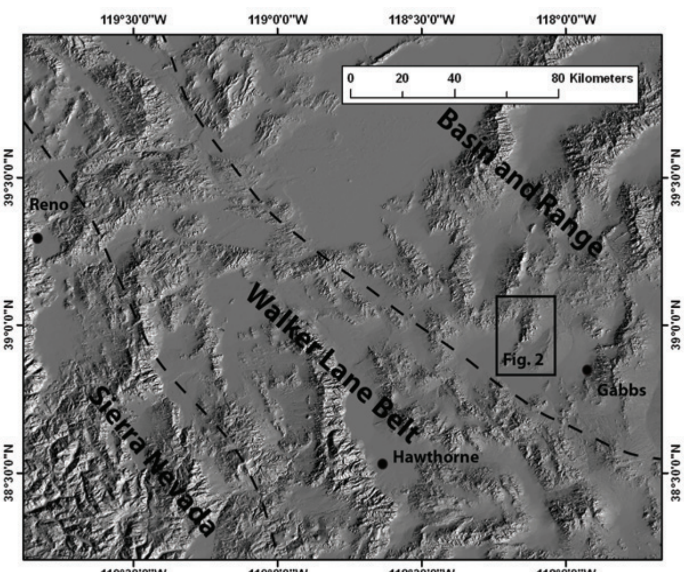

Figure 1. Hill shade generated from USGS 30 m DEM's. Major physiographic regions include the NE striking Basin and Range topography, NW striking Walker Lane Belt topography, and the Sierra Nevada. Box locates the study area and Figure 2.

The prospect area is located near Cobble Cuesta on the west side of Gabbs Valley (Figure 2). Cobble Cuesta exposes Miocene and younger fluvial, deltaic and lacustrine sedimentary rocks in a broad anticlinal fold and provide good stratigraphic and structural data (Stewart et al., 1999). Stewart et al. (1999) interprets the structure to be an anticlinal accommodation zone (Faulds and Varga, 1998) between the east-dipping faults of the Phillips Wash and East Monte Cristo fault zones, and west-dipping faults on the east side of Gabbs Valley. Bedrock exposures in the Black Hills and Monte Cristo Mountains expose Permian-Triassic sedimentary, igneous and volcanic sedimentary rocks; intruded Jurassic to Cretaceous granitic rocks; overlain unconformably by Oligocene to Miocene volcanic rocks. Fissure Ridge exposes a Miocene ash-flow fissure vent, source of the tuffs of Gabbs Valley (Ekren and Byers, 1976). The fissure complex is interpreted to be a caldera boundary and has since been faulted by younger NE trending faults of Phillips Wash. These volcanics are much too old to be a heat source but repeated eruptive events may have generated breccias associated with caldera collapse. Fractured Tertiary volcanics or Mesozoic bedrock at greater depths could provide viable reservoir rock for a geothermal system.

The 1932 Cedar Mountain earthquake (M_s = 7.2) and 1954 Fairview Peak earthquake (M_s 7.2) both generated surface ruptures

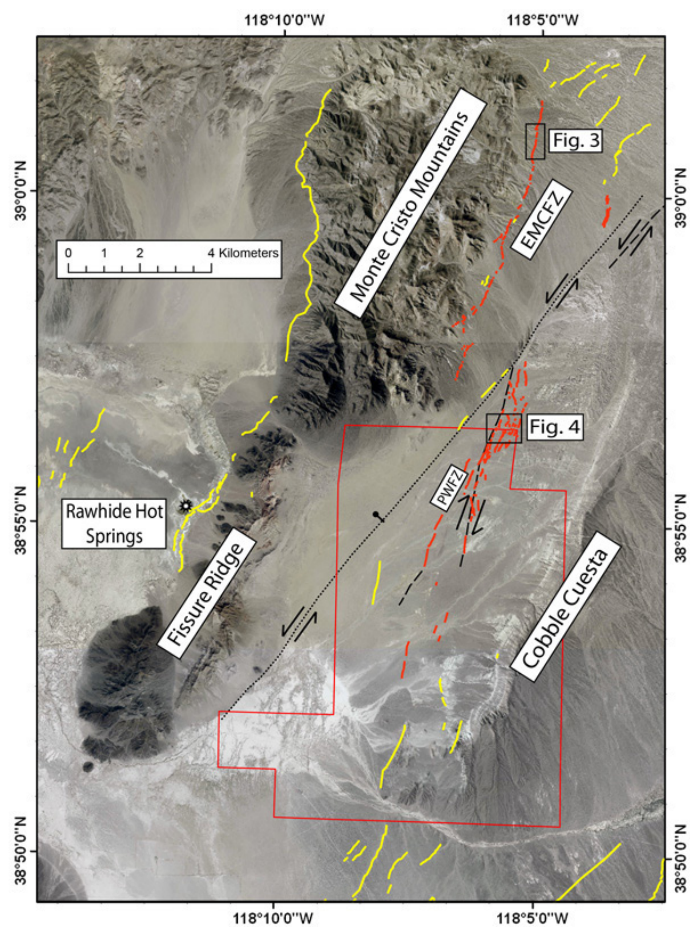

Figure 2. NAIP orthoimagery overlain by mapped faults including the Phillips Wash (PWFZ) and East Monte Cristo (EMCFZ) fault zones (Red – Historic, Yellow – Quaternary, Black – mapping by Ekren and Byers, 1986). Red polygon is GGE's Gabbs Valley geothermal lease area. Typical sites for each fault zone are shown in Figures 3 & 4.

in Gabbs Valley. These surface ruptures overlap approximately 13.5 km in Gabbs Valley. Focal mechanism solutions show dextral and dextral oblique motion on N to NNW nodal planes (Doser, 1986; Doser 1988), however, a NW trending fault is not present at the surface. The geologic slip azimuths closely resemble focal mechanism slip azimuth meaning that the overall slip azimuth was still roughly 150° (Bell et al, 2004). This suggests dextral shear is being forced onto NE striking faults or possibly a NW striking fault is at depth. The ruptures have previously been mapped using low sun-angle aerial photos and field mapping with the most detail by Caskey (1996) and Bell (1999), and reconnaissance or regional mapping by Gianella and Callahan (1934) and Ekren and Byers (1986). Fault patterns and field observations indicate left-oblique motion along the Phillips Wash fault zone (PWFZ) along a NNE trend for the 1954 ruptures (Caskey, 1996). Right-oblique motion is indicated on the Eastern Monte Cristo Mountains fault zone (EMCFZ) in NNE trend for 1932 ruptures (Caskey et al., 1996, Bell et al., 1999). These two groups of ruptures are separated by a 1.5 km left step and overlap approximately 1 km north-south (Figure 2).

Methods

In order to map active fault traces specialized imagery is necessary to provide the detail to recognize small features and offsets. Large scarps (>1 m) can be detected in conventional aerial photos, but smaller features may go undetected. The majority of scarps in Phillips Wash are <0.5 m and in sedimentary rocks or alluvium mantled by windblown sand. These conditions erode and mask small scarps concealing or obscuring their identity. Low sun-angle aerial photos and lidar (light detection and ranging) imagery are two remote sensing techniques that help enhance surface features of faulting. Low-sun-angle (LSA) aerial photos were acquired at 1:12,000 scale in 1988. LSA photos are flown in the early morning or afternoon when the sun is 10°-25° above the horizon. The low sun-angle enhances shading or illumination of the faces of scarps so they stand out against primary background textures. In addition to locating offset scarps LSA photos are also useful to identify contrasts in tone and texture that may reflect fault-controlled hydrology, and relative age of alluvial surfaces.

Lidar (light detection and ranging) swath mapping was acquired for 120,000 acres between Cobble Cuesta and the Alkali Flat west of Fissure Ridge in July 2010 for GGE by Watershed Science, Inc. Lidar provides a very detailed interpolation of the ground surface. Elevation data were gridded to a digital elevation model (DEM) with 0.5 m horizontal pixel size and better than 0.05 m vertical accuracy. DEMs were used to generate synthetic images using ArcGIS software. Hill shade images simulate the low sun-angle effect, and the high resolution of lidar data provides better resolution than LSA photos. During visual assessment of imagery the lidar is seamless to about 1: 2,000 and provides useful images to 1:500. Hill shade images were created with sun azimuth 95° and 210° to highlight the roughly NNE trend of the known faults, and to isolate scarps that do not fit this general trend. Slope shade images depict the physical topography without the bias of illumination or shade. When very low sun angles (<15°) hills and steep slopes can saturate the image leading to 'blind spots.' A slope shade image represents the steepness of the ground surface without respect to orientation. This display technique highlights slope breaks. By altering the display parameters (i.e. - histogram clips, color ramps) different features can be highlighted. A combined approach utilizing hill shade, slope shade and LSA imagery provides a variety of methods, and comparison to identify fault scarps.

In general, scarp traces are located in sediments in the basin. There are fluvial channels, active and remnant alluvial fans, and windblown sand. Fault scarps are long linear-curvilinear features that have relatively abrupt vertical separation. Additionally, these features cross-cut drainage features and do not follow contours exactly. Often, these features separate alluvial fan remnants with different drainage patterns. Bedding exposures on Cobble Cuesta and Phillips Wash trend similarly to the dominant fault trace orientation and have made identification of fault scarps ambiguous at such locations. Field mapping will be performed during summer 2011 to verify remotely sensed features. Wherever possible, fault scarps were identified in LSA, hill shade, and slope shade images to confirm a consistent presence.

Results

LSA and lidar analysis depicts two dominant fault zones (Figure 2); the Eastern Monte Cristo Mountains fault zone (EMCFZ) and the Phillips Wash fault zone (PWFZ). The EMCFZ is located in the piedmont of the Monte Cristo Mountains (Figures 2 & 3). It consists of a NNE trending series of linear features, generally less than 50 m wide, with down to the east sense of motion. These lineaments cut across alluvial fans and washes. Much of the trace is associated with scarps 0.5 to 4 m height cutting at least two dominant fan ages. Normal offsets are apparent where topographic scarps are breached by incision in the footwall due to uplift. This pattern is associated with deposition below the scarp in the hanging wall. Strike-slip motions are apparent where traces are linear, and form sags or uphill facing scarps. Many drainages are deflected or offset, and mapping has identified right-lateral movement (Bell et al., 1999; Caskey et al., 1996; this study). Our imagery depicts drainages with no offset, apparent left-offset and apparent right-offset. A typical section of the EMCFZ is shown in Figure 3. Field mapping and verification will be necessary to determine the direction of lateral offsets. Many of these scarps have historic ruptures only, while some have compound scarps recording multiple earthquakes.

The Phillips Wash fault zone is located between Phillips wash and Cobble Cuesta (Figures 2 & 4). At the southern end of the EMCFZ a ~1.5 km left step leads to the PWFZ. Wind-blown sand covers most of the PWFZ with minor fluvial deposits and limited exposure of the mid-Miocene sediments of Cobble Cuesta. The PWFZ consists of a distributed fault pattern made up of relatively short traces, spanning roughly 0.5 km wide, and loosely forming a graben. The majority of scarps face to the east while the graben is formed by a single discontinuous west facing scarp. Scarps in the PWFZ are roughly .05-0.3 m height. Possible compound scarps are much higher, but the recognition of compound scarps is difficult due to the similar strike of bedding in the sediments below. False dip slopes in strata may coincide with historic rupture, mimicking compound scarps. In the northern section, there is a dominant right stepping en echelon fault pattern that is characteristic for left-lateral motion (Withjack and Jamison, 1986). Additionally,

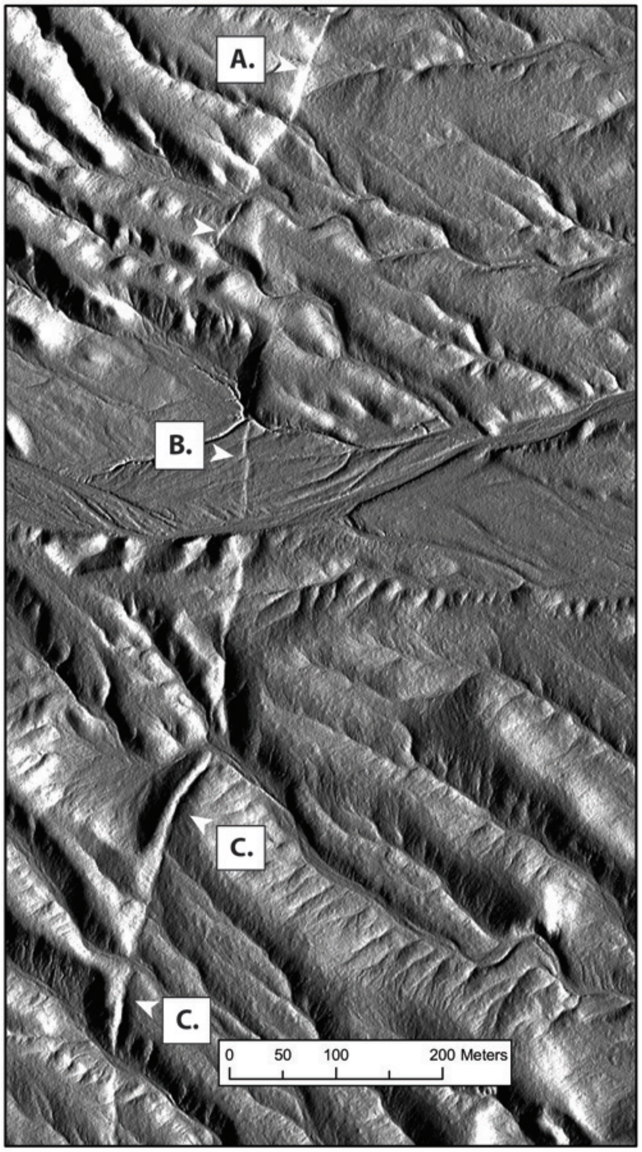

Figure 3. Hill shade image of the EMCFZ illuminated from the east with historic and compound fault scarps identified by white arrows. A. The bright lineation is a compound scarp and separates similar abandoned surfaces, and the fan surface W of the scarp is more deeply incised than to the E representing normal apparent offset. B. A younger surface is cross-cut by a single event historical scarp, small channel at arrow could indicate right-lateral offset. C. Uphill facing scarp indicates lateral motion, the channels do not depict a uniform sense of motion.

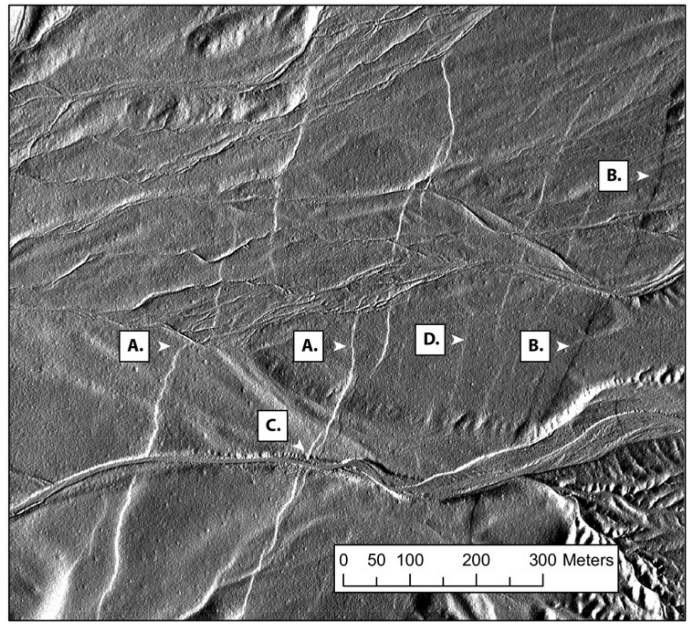

Figure 4. Hill shade image of the PWFZ illuminated from the east with historic fault scarps. Sharp, bright, NNE trending curvilinear features are east facing 1954 scarps. A. Prominent right stepping echelon pattern is evident in the left two alignments. B. Dark, sharp NNE trending features at right are west facing scarps delineating the antithetic graben. C. Location of left-lateral channel offset. D. Small potential scarps present in lidar and absent from air photos are faint light NNE lineations.

a terrace riser was mapped by Caskey having left-lateral offset. Figure 4 is a typical example of the right stepping trace pattern and broad graben.

Faulting in the piedmont alluvial fans ruptures at least three different ages of Quaternary units. Active washes are the lowest, channelized surfaces and have bar and channel morphology. Faults appear sharp and fresh with vertical separation less than 1 m. These scarps record only the historical rupture. Alluvial fan remnants of intermediate age (2+ m higher than active surfaces and lacking bar and channel morphology) have well defined fault lineaments cutting across drainages with developed scarps. Scarps cutting these abandoned fan surfaces are 0.5 to 3 m high and reflect one or more surface rupturing earthquake events. A third group of scarps is recorded in pediment surfaces overlying Miocene sediments. In Figure 2 these are located to the north and east of the EMCFZ in the top right corner where faults are yellow. These fault scarps trend NE and are east and west facing. In addition to lacking bar and channel morphology, these pediments have been incised and eroded to the point that their surface morphology is digitate, indicating that they have been inactive longer than other alluvial surfaces in the study area (Christenson and Purcell, 1985). Fault scarps are identified by uplifted alluvial surfaces, deposition patterns, and drainage patterns controlled by lineaments in fan surfaces. None of the scarps appear fresh and likely do not record historic (Holocene?) ruptures.

Discussion

We have identified two previously mapped fault zones and described their mapped orientations and characteristics. The most pertinent aspect of the work in the future will be verifying the sense of motion on these fault traces. Previous work has identified a major left-lateral fault trending NE through Phillips Wash (Ekren and Byers, 1984; Ekren and Byers, 1986). The fault appears as concealed in mapping by Ekren and Byers (1986); however adjacent the fault a 1954 splay has been mapped with right-lateral sense of slip (Figure 2). On the same splay, Caskey (1996) identified a dominant right stepping echelon pattern and an offset terrace riser for evidence of left-lateral motion on the PWFZ (Figure 4). The noted terrace riser offset could be the result of channel deflection at the scarp, degradation or erosion, and is not conclusive. The EMCFZ has previously been mapped as a right oblique normal fault (Caskey et al., 1996; Bell et al., 1999; Ekren and Byers, 1986). The major geomorphic features identify a strong normal sense of motion, with strike-slip motion secondary. Confirming these senses of motion and resolving them with potential opposite senses of motion is important to describe the current stress regime, and potential conduits for fluid movement.

The PWFZ is the dominant fault trend in the lease area and contains multiple historic fault scarps, it is the most localized example of the contemporary stress field. It is possible that left-lateral motion on the PWFZ was triggered during the Fairview Peak event and that the stress interaction of the southward movement of the Fairview Peak hanging wall in turn triggered southward movement on the PWFZ. This scenario could explain why there is little evidence in Quaternary deposits of left-lateral movement, and could negate the PWFZ's motion as dominant in the contemporary stress field. Understanding the sense of offset along the PWFZ is a major piece of evidence for developing a structural conceptual model for the potential resource.

The EMCFZ records a longer history of Quaternary faulting as depicted by the variation in size and freshness of scarps. In geologic time, the EMCFZ has recorded movement along its trace that generally reflects the WNW regional extension direction (Hammond and Thatcher, 2007). The sense of motion along this right-oblique slip fault may in turn be a better representation of the stress field, and therefore its understanding is also critical for structural conceptual modeling. The change in strike north of fault traces to NE likely records an older rupture pattern and could be reactivated differently than it was in the past, and possibly records a change in the stress field during the Quaternary.

Future work will focus on field mapping and organizing a thorough data set of evidence including slip indicators, offset features, and fault patterns. After developing a convincing argument for the current sense of slip on these structures, GPS data will be integrated to compare geologic and geodetic stress orientations.

Conclusions

Lidar and LSA photo remote sensing has provided a consistent portrait of the ground surface in the Gabbs Valley geothermal lease area. These resources have identified lineaments and active fault traces in and surrounding the lease area. The East Monte Cristo and Phillips Wash fault zones have been identified and added to. Future field work is scheduled for summer 2011 to confirm mapped features are fault rupture surface expressions. The focus of this work will be to resolve the sense of motion on the PWFZ, to collect kinematic data for integration into a structural conceptual model, and determine the relative age of Quaternary deposits that record surface ruptures. Fault motion and slip data will be used to infer the current stress regime and identify fault trends most likely to be oriented for shear and dilation based on horizontal stresses.

Acknowledgments

This work was funded by GeoGlobal Energy LLC through the DOE Geothermal Technology Program, Award No. DE-EE0002829; Recovery Act: Away from the Range Front: Intra-Basin Geothermal Exploration.

References

Al-Aquitaine Exploration, LTD (1978) Geothermal Prospect, Gabbs Valley, Nevada: unpublished consultant's report to US Department of Energy, 7.

Adams, K. D., and T.L. Sawyer (1999), Fault number 1313, Unnamed faults in Gabbs Valley, in *Quaternary fault and fold database of the United States*: U.S. Geological Survey website, http://earthquakes.usgs.gov/qfaults, accessed 04/25/2011 10:43 AM.

Bell, J. W., C. M. dePolo, A. R. Ramelli, A. M. Sarna-Wojcicki, and C. E. Meyer (1999), Surface faulting and paleoseismic history of the 1932 Cedar Mountain earthquake area, west-central Nevada, and implications for modern tectonics of the Walker Lane, *Geological Society of America Bulletin*, *111*(6), 791-807.

Bell, J. W. (2004), Pattern and Rates of Faulting in the Central Nevada Seismic Belt, and Paleoseismic Evidence for Prior Beltlike Behavior, *Bulletin of the Seismological Society of America*, *94*(4), 1229-1254.

Bell, J. W., and A. R. Ramelli (2009), Active fault controls at high-temperature geothermal sites: Prospecting for new faults, *Geothermal Resources Council Transactions*, *33*, 425-430.

Cashman, P. H., and S. A. Fontaine (2000), Strain partitioning in the northern Walker Lane, western Nevada and northeastern California, *Tectonophysics*, *326*, 111-130.

Caskey, S. J., S. G. Wesnousky, P. Zhang, and D. B. Slemmons (1996), Surface faulting of the 1954 Fairview Peak (MS 7.2) and Dixie Valley (MS 6.8) earthquakes, central Nevada, *Bulletin of the Seismological Society of America*, *86*(3), 761-787.

Christenson, G. E., and C. Purcell (1985), Correlation and age of Quaternary alluvial-fan sequences, Basin and Range province, southwestern United States, *Geological Society of America Special Papers, 203,* 115-122.

Doser, D. I. (1986), Earthquake processes in the Rainbow Mountain - Fairview Peak - Dixie Valley, Nevada, Region 1954-1959, *Journal of Geophysical Research*, *91*(B12), 12,572-12,586.

Doser, D. I. (1988), Source parameters of earthquakes in the Nevada seismic zone, 1915–1943, *Journal of Geophysical Research*, *93*(B12), 15,001–15,015.

Ekren, E. B., and F. M. Byers, Jr., (1976), Ash-flow fissure vent in west-central Nevada, *Geology*, *4*(4), 247-251.

Ekren, E. B., and F. M. Byers, Jr., (1984), The Gabbs Valley Range—A well-exposed segment of the Walker Lane in west-central Nevada, in *Western geological excursions*, Volume 4: Geological Society of America, 1984 Annual Meeting, Reno, Nevada, Field Trip Guidebook, edited by J. Lintz, 203-215.

Ekren, E. B., and F. M. Byers, Jr., (1986), Geologic map of the Mount Annie NE, Mount Annie, Ramsey Spring, and Mount Annie SE quadrangles, Mineral and Nye counties, Nevada, *USGS Miscellaneous Investigations Series*, I-1579.

Faulds, J. E., and R. J. Varga (1998), The role of accommodation zones and transfer zones in the regional segmentation of extended terranes, in *Accommodation zones and transfer zones: The regional segmentation of the Basin and Range Province, Geological Society of America Special Paper 323*, edited by J. E. Faulds and J. H. Stewart, 1-45.

Faulds, J. E., C. D. Henry, and N. H. Hinz (2005), Kinematics of the northern Walker Lane: An incipient transform fault along the Pacific–North American plate boundary, *Geology*, *33*(6), 505-508.

Gianella, P., and E. Callaghan (1934), The Cedar Mountain, Nevada, Earthquake of December 20, 1932, *Bulletin of the Seismological Society of America*, *24*(4), 378-384.

Hammond, W. C., and W. Thatcher (2007), Crustal deformation across the Sierra Nevada, northern Walker Lane, Basin and Range transition, western United States measured with GPS, 2000–2004, *Journal of Geophysical Research*, *112*(B5), 1-26.

Moeck, I., G. Kwiatek, and G. Zimmermann (2009), Slip tendency analysis, fault reactivation potential and induced seismicity in a deep geothermal reservoir, *Journal of Structural Geology*, *31*(10), 1174-1182.

Moeck, I., N. Hinz, J. Faulds, J. Bell, A. Kell-Hills, and J. Louie (2010), 3D Geological Mapping as a New Method in Geothermal Exploration : A Case Study from Central Nevada, *Geothermal Resources Council Transactions*, *34*, 807-811.

Stewart, J. H. (1978), Basin-range structure in western North America: A review, in *Cenozoic tectonics and regional geophysics of the western cordillera*, edited by R. Smith and G. Eaton, pp. 1-31, Geological Society of America.

Stewart, J. H. (1988), Tectonics of the Walker Lane Belt, Western Great Basin, in *Metamorphism and Crustal Evolution of the Western United States*, edited by W. G. Ernst, pp. 683-713.

Stewart, J. H., A. M. Sarna-Wojcicki, C. E. Meyer, and E. Wan (1999), Stratigraphy, tephrochronology, and structural setting of Miocene sedimentary rocks in the Cobble Cuesta area, west-central Nevada, *USGS Open File Report* (99-352), 21.

Wesnousky, S. G. (2005), Active faulting in the Walker Lane, *Tectonics*, *24*(3), 1-35.

Withjack, M. O., and W. R. Jamison (1986), Deformation Produced by Oblique Rifting, *Tectonophysics*, *126*(2-4), 99–124.